Dish-Shape Magnetic Flux Concentrator for Inductive Power Transfer Systems

Marwan H. Mohammed[1], Yasir M. Y. Ameen[1], and Ahmed A. S. Mohamed[2]
[1] Department of Electrical Engineering, University of Mosul, Iraq
[2] National Renewable Energy Laboratory (NREL), Golden, CO 80401-3393, USA
Email: Mar600r@gmail.com; yasir_752000@uomosul.edu.iq; Ahmed.Mohamed@nrel.gov

***Abstract*—Recently, safety concerns related to electro-magnetic fields (EMFs) in inductive power transfer (IPT) systems for electric vehicles applications are pointed out. Magnetic flux concentrators are commonly used in the system to direct magnetic field lines and enhance the power transfer capability and efficiency. This article explores the performance of an IPT system for two different shapes of magnetic flux concentrators in terms of magnetic field distribution and power transmission efficiency. The dish-shape and plate-shape flux concentrators are examined and compared with a coreless IPT system. A simulation study based on three-dimensional finite-element analysis is carried out to design the magnetic couplers and analyze the IPT system's performance. The simulation results are verified analytically and good matches are achieved.**

***Index Terms*—Inductive Power Transfer (IPT), magnetic flux concentrator, magnetic field distribution, power transfer efficiency, Wireless Power Transfer (WPT)**

I. Introduction

Nikola Tesla dreamed of a ''wireless world'' at the end of the last century [1]. In fact, we, as researchers, have a dream of providing electrical energy wirelessly through the air as well. The dream has come true recently, as many applications today are based on Wireless Power Transfer (WPT) technology, including medical devices, cell phones, laptops, home appliances and Electric Vehicles (EVs). Therefore, massive attention has been given to improve the performance of WPT systems, which is typically measured by the Power Transmission Efficiency (PTE) and the compatibility with the safety requirements [2]-[6]. On this basis, the Inductive Power Transmission System (IPTS) is one of the best-known WPT technologies that offers the best performance for high-power applications, such as EV charging. It consists of two electrically isolated sides. Each side consists of a power converter, a compensation network, and a power pad. The power transfer from a primary coil (in the road) to a secondary coil (in the vehicle) by magnetic induction while the system operating at resonance [7]. The PTE depends on the coupling coefficient between the two coils (k) and the quality factor of each coil, which is related to the coil's parameters (inductance and resistance) and resonant frequency (f) [8]-[10]. Consequently, the magnetic coupler should be designed to provide high coupling and quality factors to meeting the power transfer requirement [11]. Typically, an inductive pad consists of a copper Litz wire that carries the high-frequency current, a magnetic core for directing the flux lines from the transmitter toward the receiver, and an aluminum shielding plate for limiting the leakage flux around the system. Spiral planar coils are typically used in the system to reduce the pad thickness and increase the flux loops' travel distance. The magnetic core is placed behind the spiral coils to reduce the magnetic path reluctance, enhance the coupling performance, reduce the leakage flux and thus increase the values of both k and PTE. Exposure to high-frequency EMFs presents a safety concern that has the potential to cause health problems for humans and living objects in the long-term. Therefore, the International Commission on Non-Ionizing Radiation Protection (ICNIRP) and the World Health Organization (WHO) have attested and issued some guidelines to ensure the safety of the living objects [12], [13]. For an IPT system to meet these safety requirements, leakage EMFs around the system should be suppressed. For EV inductive charging applications, more attention should be paid to the problem related to exposure to magnetic fields due to the high-power operation and large airgap (10-40 cm) [7], [14]-[16]. Fig. 1 shows the structure of a typical EV inductive charger along with the distribution of magnetic fields around the transmitter and receiver coils. As it can be noticed, a significant portion of both leakage and coupled EMFs extend around the system and may present a safety issue if they exceed the standard limits.

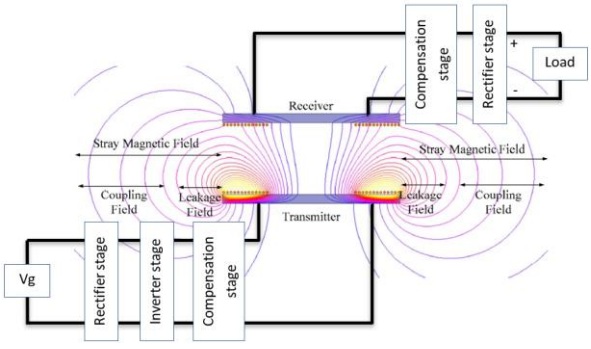

Fig. 1. Structure and operation of an IPT system.

Different types of EMF shielding techniques are presented in the literature: passive, active and reactive

Manuscript received February 11, 2020; revised April 15, 2020; accepted April 29, 2020.
Corresponding author: Marwan H. Mohammed (mar600r@gmail.com).

doi: 10.18178/ijeetc.9.6.455-461

shielding, as indicated in Fig. 2 [17]-[19]. Passive shields show an effective performance for low-power chargers (<50 kW), which can be either a magnetic core, conductive plate or both [20]-[24]. Magnetic core is typically made of a high permeability material such as ferrite to concentrate and confine the magnetic flux between the coils [18], [19], [25]-[27]. Another fact is that the coil shape has significant impact on the system performance and leakage flux. Several coil shapes are proposed, investigated and compared in the literature; however, circular and square coils are the most commonly used due to their simple structure and high EMF [28]. Several researches have been conducted considering the different shapes of the magnetic core for the circular coil. In [29] and [30], a convex-magnetic flux concentrator was proposed in [22], which shows a significant reduction in the magnetic leakage flux and consequently increasing the coupling performance.

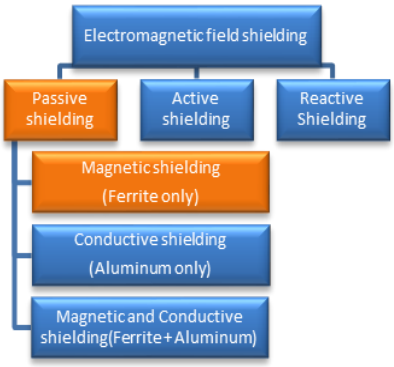

Fig. 2. Types of EMFs shielding for IPT systems.

Different from the abovementioned studies, this paper proposes a dish-shape magnetic flux concentrator for the circular pad. It investigates its performance compared to the plate-shape and an air-core coil in terms of coupling factor, PTE, and leakage EMFs. Both dish-shape and plate-shape flux concentrators are made of ferrite. Three-dimensional (3D) finite-element models (FEMs) for the different shapes are developed and analyzed using Ansys Maxwell software. In addition, circuit models for the entire system, including coupler, power converters, and series-series compensation networks are developed and evaluated in the same environment. Both FEMs along with circuit-based models are utilized to design and optimize the proposed dish-shape flux concentrator.

II. Numerical Modeling of Inductive Coupler

A simulation study based on finite element analysis (FEA) has been used to model, design, and analyze the IPT system. The geometric design and the flux distribution analysis of the inductive coils and their magnetic flux concentrators have been carried out with the Ansys Maxwell tool. The coils' parameters are extracted from FEA and inserted into a circuit-based model in Ansys Simplorer to analyze the entire system's performance, considering power converters, compensation networks, and battery load.

A. Design of the Magnetic Coupler Circuit

As stated, the utilization of the ferrite core along with aluminum plate significantly reduces the leakage flux and improve the system's performance [16]. Another important factor that impacts both *k* and EMFs is the shape of the pad. Several shapes pad are presented and analyzed in the literature, which can be classified into Non-Polarized Pads (NPP) and polarized pads (PPs). NPPs consists of a single coil that generates vertical flux components, such as circular (CP) and rectangular (RP) pads. PPs consist of multiple-coil that generate both horizontal and vertical flux components, such as Double-D (DD), Double-D Quadrature (DDQ), bipolar (BP) and Quadruple-D pad [31]. These shapes are presented in Fig. 3 and compared in [3] and [32] in terms of design and applications.

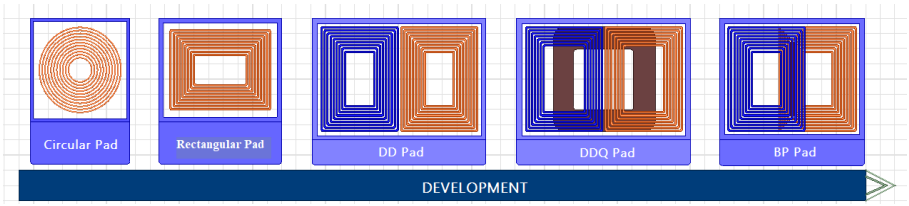

Fig. 3. Pad structures for IPT system.

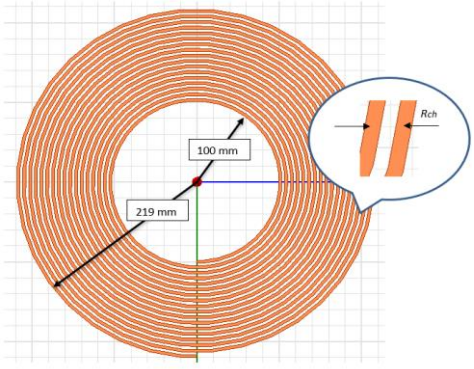

Fig. 4. Geometry of CP coil.

Table I: Design Parameters of the Helix CP Coil

Coil Parameter	Value
Polygon radius	2.5 mm
Coil inner radius	100 mm
Turns space, R_{ch}	7 mm
Number of turns	17

The circular structure is considered in this paper for simplicity and maturity. The copper coil is modeled as stranded with large number of strands to emulate Litz wire. Rectangular cross-section is considered for modeling the coil to reduce the computational effort, as indicated in Fig. 4. The consists of 17 turns with an inner and outer radius of 100 mm and 219 mm, respectively, as described in Table I. Both transmitter and receiver coils are identical.

The CP is easy to develop and offers the same tolerance for misalignment in all directions. In addition, it offers the best coupling during the perfect alignment case [26].

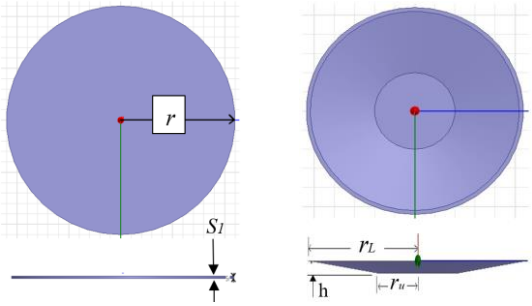

(a) (b)

Fig. 5. Magnetic flux concentrators (a) Plate-shape design. (b) Dish-shape design.

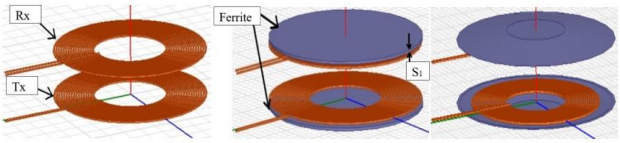

(a) (b) (c)

Fig. 6. Magnetic coupler structure: (a) air-core concentrator, (b) conventional plate-shape concentrator, and (c) dish-shape concentrator.

TABLE II: DESIGN PARAMETERS OF THE CONCENTRATORS

Plate-shape design		Dish-shape design	
Parameter	Value (mm)	Parameter	Value (mm)
Shielding radius (r)	220	Outer radius (ru)	100
Shield thickness (S_1)	3	Lower radius (r_L)	270
Gap between shield and coil (g)	5	Height (h)	15
Material	Ferrite	Material	Ferrite
		Thickness (S_2)	3

The plate-shape and dish-shape magnetic flux concentrators with ferrite material are designed and presented in Fig. 5 (a) and (b), respectively. As it can be noticed, the plate shape is just a flat circular sheet of ferrite with a radius r, while the dish shape has a small flat sheet with radius r_L surrounded by a tilted one with an outer radius of r_U. The dimensions and characteristics of both shapes are presented in Table II. The final coupler designs considering three cases of flux concentrators are presented in Fig. 6. The figure shows the air-core pad, conventional plate-shape pad, and the proposed dish-shape pad.

B. Compensation Topologies

An effective and efficient power transmission in IPT systems requires compensation for the large leakage inductance due to the large air-gap. Resonance network is typically added to the transmitter and receiver circuits for this purpose. Four compensation topologies are mainly used in IPT systems: Series-Series (SS), Series-Parallel (SP), Parallel-Series (PS), and Parallel-Parallel (PP), as depicted in Fig. 7. SS topology is considered in this work due to its simplicity in design, and control, which does not depend on k and load conditions [26], [33].

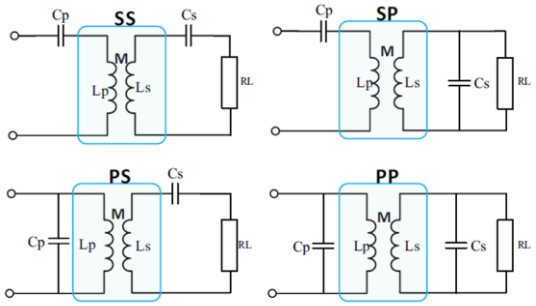

Fig. 7. Compensation topology

III. PERFORMANCE ANALYSIS OF IPT SYSTEM

The simulation circuit diagram developed in ANSYS Simplorer is directly linked to the magnetic coupler structure created in the Maxwell environment, as indicated in Fig. 8. In fact, FEA in Maxwell provides the values of the coils' self-inductance, coupling coefficient, and mutual inductance to carry out the simulation of the IPT system. The system overall efficiency is estimated for the three magnetic couplers given before with an air gap of 150 mm. The input supply voltage and load resistance are selected to be V_s=50V, and R_L=7Ω, respectively. Whereas the values of the compensator capacitors for the both sides C_p and C_s are calculated based on the resonant frequency and self-inductance using (1).

$$f_0 = \frac{1}{2\pi\sqrt{L_p C_p}} = \frac{1}{2\pi\sqrt{L_s C_s}} \quad (1)$$

The resonant frequency is set to be f_o=85 kHz, and the IPT circuit parameters are shown in Table III.

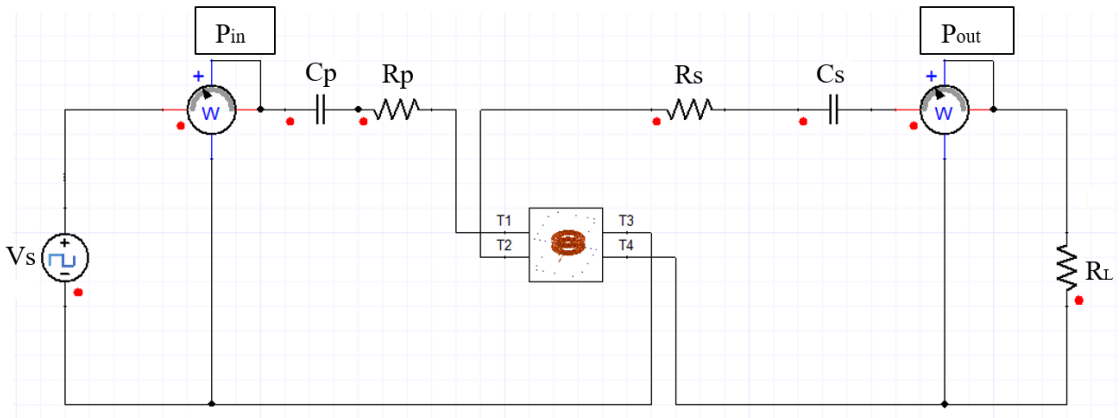

Fig. 8. Circuit diagram of IPT system.

TABLE III: WPT CIRCUIT PARAMETERS

Parameters	Air-core	Plate-shape concentrator	Dish-shape concentrator
Primary coil resistance, R_p	0.178 Ω	0.178 Ω	0.178 Ω
Secondary coil resistance, R_s	0.178 Ω	0.178 Ω	0.178 Ω
Primary side capacitor, C_p	31.78 nF	20 nF	18.7 nF
Secondary side capacitor, C_s	31.78 nF	20 nF	18.7 nF

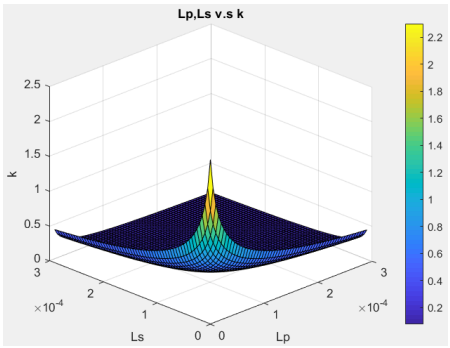

(a)

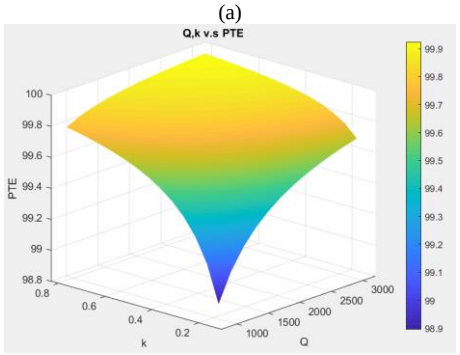

(b)

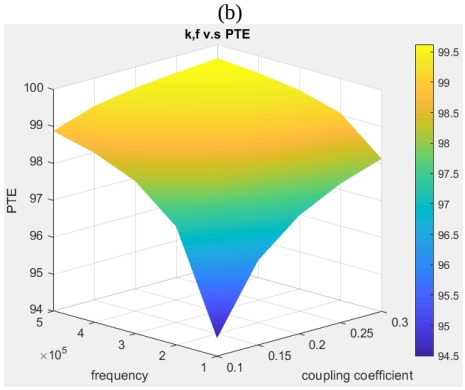

(c)

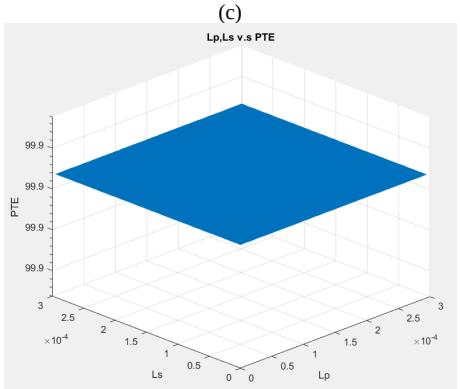

(d)

Fig. 9. (a) The variation of k with L_p and L_s. (b) The relation of PTE with k and Q. (c) The effect of M and the resonant frequency (w) on the PTE. (d) The relation of PTE with L_p and L_s.

A simulation analysis is performed for measuring the input power (P_{in}) and output power (P_{out}) to find out the efficiency of the IPT system. The maximum achievable efficiency can be expressed mathematically by (2) [3].

$$\eta_{\max} = k^2 Q_P Q_s \Big/ \left(1+\sqrt{1+k^2 Q_p Q_s}\right)^2 \quad (2)$$

where k is the coupling coefficient between coils, Q_p, Q_s are quality factor of transmitter and receiver respectively.

The relation between k and the mutual inductance is given as follows

$$k = M \Big/ \sqrt{L_p L_s} \quad (3)$$

The quality factors (Q_p and Q_s) of the coils are related to their parasitic resistances and self-inductances, as described by (4).

$$Q_p = \frac{w_0 L_p}{R_p}, \quad Q_s = \frac{w_0 L_s}{R_s} \quad (4)$$

where w_0 is the angular resonant frequency.

Substituting (3) and (4) in (2), the following equation is yield:

$$\eta_{\max} = \frac{M^2 w_o^2}{R_p R_s} \Big/ \left(1+\sqrt{1+\frac{M^2 w_o^2}{R_p R_s}}\right)^2 \quad (5)$$

According to (5), it can be concluded that the transmission efficiency is related to M, W_0, R_p, and Rs. The above presented equations are depicted in Fig. 9. Where, Fig. 9 (a) represents (3) for the variation of k with L_p and L_s. Whereas, Fig. 9 (b) illustrates the relation of PTE with k and Q according to (2). Fig. 9 (c) shows the effect of M and the resonant frequency (w) on the PTE based on (5). The correlation-free between the PTE with both L_p and L_s has appeared in Fig. 9 (d).

IV. RESULTS AND DISCUSSION

The following sections highlight the results achieved and list some of the interpretations.

A. Analysis of Magnetic Field Distributions by FEM

As indicated by the ICNIRP standard for WPT emissions testing instructions, the magnetic field limit is 27μTrms for general-public exposure and 15μTrms in areas where body-implanted pacemakers are an Interest [12]. Table IV presents the reference levels for the EMFs defined by the different standards [11].

TABLE IV: STANDARD REFERENCE LEVELS OF EMFS EXPOSURE

Standard	Magnetic field, B_{rms} (μT)		Electric field, E_{rms} (V/m)	
	General public	Occupa-tional	General public	Occupati-onal
ICNIRP 2010 (1 Hz – 100 KHz)	27	100	83	170
IEEE C.95.1 2014 (3KHz–5 MHz)	205	615	614	1842
ACGIHTLV 2017 (2.5-30) KHz	---	200	---	1842

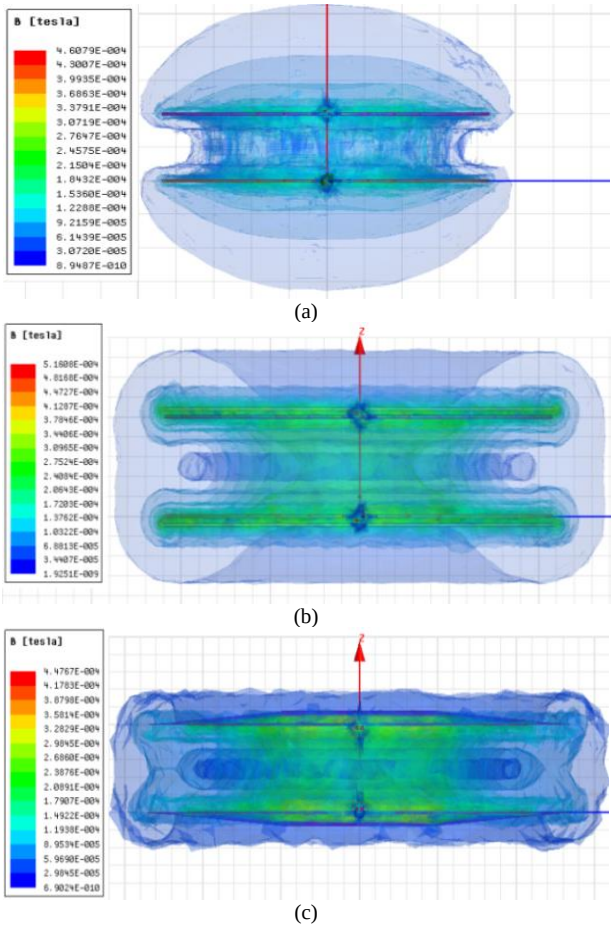

(a) (b) (c)

Fig. 10. Magnetic field distributions analysis of the magnetic coupler: (a) Without concentrator, (b) With traditional plate-shape concentrator, and (c) With dish-shape concentrator.

TABLE V: VARIATION OF *L*, *M*, AND *K* VALUES WITH THE AIR-GAP

Parameter	Without concentrator			Traditional concentrator			Dish concentrator		
Air-gap (mm)	**100**	**150**	**200**	**100**	**150**	**200**	**100**	**150**	**200**
Primary Self-inductance (L_p_μH)	110.3	110.4	110.04	182.55	174.74	172.2	199.39	187.15	183.67
Secondary Self-inductance (L_s_μH)	110.3	110.4	110.21	182.52	174.68	172.23	201	188.73	185.27
Mutual Inductance (M_μH)	36.41	23	15.126	80	47.05	29.25	94.73	55.126	34.21
Coupling Coefficient (K)	0.33	0.208	0.137	0.438	0.269	0.169	0.473	0.293	0.185

The magnetic field distributions for the magnetic coupler circuit with and without flux concentrators are shown in Fig. 10. For the coils without concentrator structure, there is a sturdy magnetic field distribution around the non-effective transmission area as shown in Fig. 10 (a). For the second case, the use of the plate-shape flux concentrator reduces the divergence of the magnetic field in the non-effective transmission area and focuses most of the magnetic flux in a targeted direction as shown in Fig. 10 (b). Whereas the use of the dish-shape flux concentrator is focusing the field at the center and minimizing the leakage flux from the coils shown in Fig. 10(c).

The results of the variance for the *L*, *M* and *k* values with the air gap for the three cases (as shown in Fig.6) are presented in Table V.

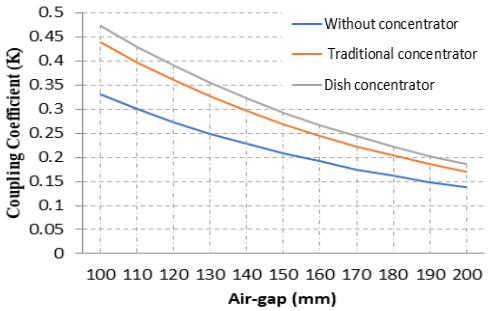

Fig. 11. The variation of the *k* coefficient with the air-gap

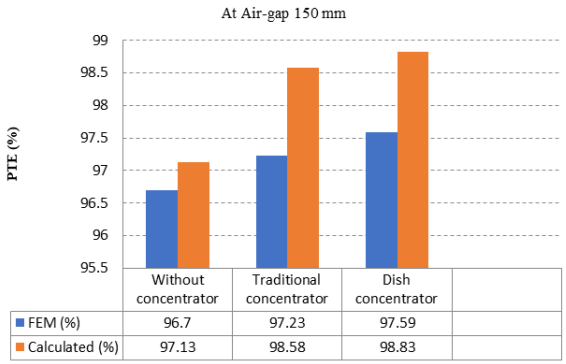

	Without concentrator	Traditional concentrator	Dish concentrator
FEM (%)	96.7	97.23	97.59
Calculated (%)	97.13	98.58	98.83

Fig. 12. FEA results and the calculated results of PTE for the three cases.

Fig. 11 depicts the variation of the *k* coefficient with the air-gap for the three presented cases. While, Fig. 12 shows both the FEA simulation results and the analytically calculated results of PTE for the above cases at air-gap equal to 150 mm. The PTEs are almost the same with a small gain for the dish-shape magnetic flux concentrator, but the latter case is preferred for safety reasons.

V. CONCLUSION

This paper presented a dish-shape magnetic flux concentrator for circular pad in inductive charger for electric vehicles. A complete design procedure for various magnetic couplers with and without flux concentrators has been carried out based on 3D FEA. The system performance with the proposed dish-shape flux concentrator has been compared with that with the conventional plate-shape concentrator. The results show the dish-shaped concentrator provides less EMFs around the system, which allows the system to meet the safety requirements defined by the international guidelines. In addition, it shows a higher coupling performance than the plate-shaped concentrator. This is because of the ability of the dish-shaped concentrator to direct the magnetic flux lines toward the center of the receiver pad. However, the main challenges for the proposed system are that the difficulty of implementation, as it requires special cuts for the magnetic material. This difficulty can be overcome by approximating the shape, considering the commercially available blocks.

CONFLICT OF INTEREST

The authors declare no conflict of interest.

AUTHOR CONTRIBUTIONS

Marwan H. Mohammed conducted the research and wrote the paper; Dr. Yasir M.Y. Ameen and Dr. Ahmed A. S. Mohamed both made the necessary adjustments and analyzed the data; all authors had approved the final version.

ACKNOWLEDGMENT

The authors thank the University of Mosul and the supervisors who supported this effort. The National Renewable Energy Laboratory (NREL) is the current address for the third author only. NREL and the U.S. Department of Energy (DOE) did not contribute to this work.

REFERENCES

[1] Naoki Shinohara, *Wireless Power Transfer*, 1st ed. London: IET Digital Library, ch.1, 2018, pp. 1-2.

[2] W. Zhang and C. C. Mi, "Compensation topologies of high-power wireless power transfer systems," *IEEE Trans. Veh. Technol.*, vol. 65, no. 6, pp. 4768–4778, 2016.

[3] Z. Zhang, H. Pang, A. Georgiadis, and C. Cecati, "Wireless power transfer - an overview," *IEEE Trans. Ind. Electron.*, vol. 66, no. 2, pp. 1044–1058, 2019.

[4] S. Li and C. C. Mi, "Wireless power transfer for electric vehicle applications," *IEEE J. Emerg. Sel. Top. Power Electron.*, vol. 3, no. 1, pp. 4–17, 2014.

[5] S. Zhang, J. Wu, and S. Lu, "Collaborative mobile charging," *IEEE Trans. Comput.*, vol. 64, no. 3, pp. 654–667, 2015.

[6] B. Griffin and C. Detweiler, "Resonant wireless power transfer to ground sensors from a UAV resonant wireless power transfer to ground sensors from a UAV," presented at 2012 IEEE Int. Conf. on Robotics and Automation, 2012.

[7] A. A. S. Mohamed and O. Mohammed, "Bilayer predictive power flow controller for bidirectional operation of wirelessly connected electric vehicles," *IEEE Trans. on Industry Applications*, vol. 55, no. 4, pp. 4258-4267, July-Aug. 2019.

[8] A. A. S. Mohamed, S. An, and O. Mohammed, "Coil design optimization of power pad in ipt system for electric vehicle applications," *IEEE Trans. Magn*., vol. 54, no. 4, pp. 1–5, 2018.

[9] D. H. Tran, V. B. Vu, and W. Choi, "Design of a high-efficiency wireless power transfer system with intermediate coils for the on-board chargers of electric vehicles," *IEEE Trans. Power Electron*., vol. 33, no. 1, pp. 175–187, 2018.

[10] J. Y. Lee and B. M. Han, "A bidirectional wireless power transfer EV charger using self-resonant PWM," *IEEE Trans. Power Electron*., vol. 30, no. 4, pp. 1784–1787, 2015.

[11] F. Wen and X. Huang, "Optimal magnetic field shielding method by metallic sheets in wireless power transfer system," *Energies*, vol. 9, no. 9, p. 733, Sep. 2016.

[12] A. A. S. Mohamed, S. Member, A. Meintz, P. Schrafel, and A. Calabro, "Testing and assessment of EMFs and touch currents from 25-kW IPT system for medium-duty EVs," *IEEE Trans. on Vehicular Technology*, vol. 68, no. 8, pp. 7477-7487, Aug. 2019.

[13] M. Mohammad, J. Pries, O. Onar, *et al*., "Design of an EMF suppressing magnetic shield for a 100-kW DD-coil wireless charging system for electric vehicles," in *Proc. IEEE Applied Power Electronics Conference and Exposition (APEC)*, 2019, pp. 1521-157.

[14] V. Cirimele, F. Freschi, L. Giaccone, L. Pichon, and M. Repetto, "Human exposure assessment in dynamic inductive power transfer for automotive applications," *IEEE Trans. Magn*., vol. 53, no. 6, pp. 1–4, Jun. 2017.

[15] H. H. Wu, A. Gilchrist, K. D. Sealy, and D. Bronson, "A high efficiency 5 kW inductive charger for EVs using dual side control," *IEEE Trans. Ind. Informatics*, vol. 8, no. 3, pp. 585–595, 2012.

[16] R. Mai, Y. Liu, Y. Li, P. Yue, G. Cao, and Z. He, "An active-rectifier-based maximum efficiency tracking method using an additional measurement coil for wireless power transfer," *IEEE Trans. Power Electron*., vol. 33, no. 1, pp. 716–728, 2018.

[17] T. Campi, S. Cruciani, F. Maradei, and M. Feliziani, "Active coil system for magnetic field reduction in an automotive wireless power transfer system," in *Proc. IEEE Int. Symp. Electromagn. Compat. Signal Power Integr.*, 2019, pp. 189–192.

[18] J. Park, D. Kim, K. Hwang, H. H. Park, S. I. Kwak, J. H. Kwon, and S. Ahn, "A resonant reactive shielding for planar wireless power transfer system in smartphone application," *IEEE Trans. on Electromagnetic Compatibility*, vol. 59, no. 2, pp. 695–703, April 2017.

[19] S. Kim, H. H. Park, J. Kim, J. Kim, and S. Ahn, "Design and analysis of a resonant reactive shield for a wireless power electric vehicle," *IEEE Trans. Microw. Theory Tech*., vol. 62, no. 4, pp. 1057–1066, 2014.

[20] A. A. S. Mohamed, A. A. Shaier, H. Metwally, and S. I. Selem, "A comprehensive overview of inductive pad in electric vehicles stationary charging," *Appl. Energy*, vol. 262, Jan.2020.

[21] K. Aditya and S. S. Williamson, "Design guidelines to Avoid bifurcation in a series – series compensated inductive power transfer system," *IEEE Trans. Ind. Electron*., vol. 66, no. 5, pp. 3973–3982, 2019.

[22] Z. Dai, J. Wang, M. Long, H. Huang, and M. Sun, "Magnetic shielding structure optimization design for wireless power transmission coil," *AIP Adv*., vol. 7, no. 9, pp. 1–13, 2017.

[23] F. Wen and X. Huang, "Human exposure to electromagnetic fields from parallel wireless power transfer systems," *Int. J. Environ. Res. Public Health*, vol. 14, no. 2, p. 157, Feb. 2017.

[24] T. Batra and E. Schaltz, "Passive shielding effect on space profile of magnetic field emissions for wireless power transfer to vehicles," *Journal of Applied Physics*, vol. 117, no. 17A739, pp. 1-2, 2015.

[25] Z. Bi, T. Kan, C. C. Mi, Y. Zhang, Z. Zhao, and G. A. Keoleian, "A review of wireless power transfer for electric vehicles: Prospects to enhance sustainable mobility," *Appl. Energy*, vol. 179, pp. 413–425, 2016.

[26] K. Eldin, I. Elnail, L. Huang, L. Tan, S. Wang, and X. Wu, "Resonant reactive current shield design in WPT systems for charging EVs," in *Proc. IEEE PES Asia-Pacific Power and Energy Engineering Conf*., 2018, pp. 56–59.

[27] H. Kim, J. Cho, S. Ahn, J. Kim, and J. Kim, "Suppression of leakage magnetic field from a wireless power transfer system using ferrimagnetic material and metallic shielding," in *Proc. IEEE Int. Symp. Electromagn. Compat.*, Aug. 2012, pp. 640–645.

[28] Z. Bi, T. Kan, C. C. Mi, Y. Zhang, Z. Zhao, and G. A. Keoleian, "A review of wireless power transfer for electric vehicles: Prospects to enhance sustainable mobility," *Appl. Energy*, vol. 179, pp. 413–425, 2016.

[29] A. Dolara, S. Leva, M. L. F. C. Dezza, and M. Mauri, "Coil design and magnetic shielding of a resonant wireless power transfer system for electric vehicle battery charging" in *Proc. IEEE 6th Int. Conf. on Renewable Energy Research and Applications (ICRERA)*, 2017, pp. 200-205.

[30] M. Lu and K. D. T. Ngo, "Systematic design of coils in series–series inductive power transfer for power transferability and efficiency," *IEEE Trans. on Power Electronics*, vol. 33, no. 4, pp. 3333-3345, 2017.

[31] A. Ahmad, M. S. Alam, and A. A. S. Mohamed, "Design and interoperability analysis of quadruple pad structure for electric vehicle wireless charging application," *IEEE Trans. Transport. Electrific.*, vol. 5, no. 4, pp. 934–945, 2019.

[32] A. Ahmad, M. S. Alam, and R. Chabaan, "A comprehensive review of wireless charging technologies for electric vehicles," *IEEE Trans. Transport. Electrific*., vol. 4, no. 1, pp. 38–63,2017.

[33] C. Panchal, S. Stegen, and J. Lu, "Review of static and dynamic wireless electric vehicle charging system," *Engineering Science*

and Technology, An International Journal, vol. 21, no. 5, pp. 922–937, 2018.

Marwan H. Mohammed received the B.Sc. degrees from the Electrical Power and Machines Department, Mosul University, Iraq, in 2014, where he is currently pursuing his M.Sc. degree in power electronics. His current research interests include the design and analysis of wireless power transfer systems.

Dr. Yasir M. Y. Ameen received bachelor, master, and Ph.D. degree in Power and Electrical Machines Engineering from University of Mosul in 1997, 2000, and 2008 respectively. He is a member in Iraqi Engineers Union (IEU). He is a Lecturer in Department of Electrical Engineering. His research interests include power electronics, electrical machines and their drives. His affiliation is Department of Electrical Engineering, College of Engineering, University of Mosul, Mosul, 41001, Iraq. Email: yasir_752000@uomosul.edu.iq, Mobile: +964- 770-164-0663.

Dr. Ahmed A. S. Mohamed received his B.Sc. (2008) and M.Sc. (2012) degrees in Electrical Engineering from the Electrical Power and Machines Department, ZU, Egypt. He finished his Ph.D. degree in Electrical Engineering at FIU, Miami, FL, USA, in December 2017. Dr. Mohamed is currently a Research Engineer at the National Renewable Energy Laboratory (NREL), Golden, CO 80401-3393, USA. From 2008 to 2013, Dr. Mohamed served as a faculty member at ZU, Egypt. His research focus on electric vehicle wireless charging, power electronics, transportation electrification, as well as PV power systems. Dr. Mohamed is a Senior IEEE member and he was a recipient of the Outstanding Doctoral Student Award in fall 2017 from FIU.